

The distribution of kinetic energy in the Southern Ocean: a comparison between observations and an eddy resolving general circulation model

DAVID P. STEVENS¹ AND PETER D. KILLWORTH²†

¹*School of Mathematics, University of East Anglia, Norwich NR4 7TJ, U.K.*

²*Institute of Oceanographic Sciences, Deacon Laboratory, Wormley, Godalming, Surrey GU8 5UB, U.K.*

SUMMARY

It is widely believed from model studies that the transient eddy field plays an important role in the dynamics of the Southern Ocean. Accordingly, the distribution and partition of kinetic energy from an eddy resolving general circulation model of the Southern Ocean is compared with existing non-altimetric observations. Good agreement in distribution is found with some of the more recent observations. The amplitudes of the model energies, while for the most part well correlated with observations, are significantly lower than those observed (although observations differ greatly in their estimates). This reduction of energy is in agreement with other recent eddy resolving models, and is partly caused by the lack of correctly varying wind and buoyancy forcing, together with inadequate representation of instability processes. Nevertheless, the correlations suggest that the model results may be used as a proxy for reality in many circumstances.

1. INTRODUCTION

The dynamics of the Antarctic Circumpolar Current (ACC) are far from well understood. Simple theories of the current (e.g. Johnson & Bryden 1989), eddy-resolving quasi-geostrophic models (Wolff *et al.* 1991) and eddy-resolving primitive equation models (FRAM Group 1991) all imply that the transient eddy field plays an important role in the dynamics of the ACC. Accordingly, it is important that models reproduce an eddy field which is in some sense in agreement with the observed field. Since the initial work of Wyrтки *et al.* (1976) there have been a number of attempts to map the distribution of kinetic energy over the world ocean and in particular the Southern Ocean. If a good data base of observations is built up it will be useful for testing four-dimensional eddy resolving general circulation models (ERGCMs).

It is the purpose of this article to compare and enhance existing descriptions of kinetic energy distributions with results from the U.K. Fine Resolution Antarctic Model (FRAM). A detailed description of the model can be found in the article by the FRAM group (1991), and a comprehensive survey of its early results in Webb *et al.* (1991).

Wyrтки *et al.* (1976) used observations of surface drift currents made by merchant ships to calculate both mean and eddy kinetic energy. The map for the world oceans was produced on five degree squares. There are few shipping routes in the Southern Ocean,

leading to a paucity of data, both spatial and temporal, in that region. Although the grid size used is large, high values of kinetic energy can still be found in the region of western boundary currents and the Drake Passage, plus a suggestion of eddy activity to the east of the Agulhas retroflexion.

More recently a number of researchers (Patterson 1985; Daniault & Ménard 1985; Piola *et al.* 1987) have examined data from drifting buoys deployed during the First GARP Global Experiment (FGGE). The results from these studies are all comparable, as is to be expected. Grids on the scale of four to five degrees are used, thus giving rather poor spatial resolution. Improving the resolution reduces the number of observations in most ocean areas to an unacceptable level (but see Patterson (1985) for localized regions such as the Macquarie Ridge). The temporal resolution is very good, as many as 16 fixes per buoy per day being possible. The results from the above studies are in broad qualitative agreement with Wyrтки *et al.* (1976). A difficulty is that drifters tend to 'band' into frontal zones (Johnson 1989), thus giving biased estimates of flow speeds and energies.

In the last decade, enough long-term current meter moorings have been made that estimates of mean and eddy kinetic energy can be made at certain locations (collected by Dickson (1990)). These moorings were chosen, it must be admitted, to lie in regions deemed scientifically interesting; which brings with it a bias in information. The advantage of these data is that they provide information on depth variability of the energy fields, which most historical drifters do not.

This paper will directly compare these data with

† Present address: Robert Hooke Institute, The Observatory, Parks Road, Oxford OX1 3PU, U.K.

the FRAM results. There are, of course, many possible ways to make comparisons which are not carried out here (e.g. spectral analysis in space or time, as carried out for the Community Modelling Effort N. Atlantic (CME) calculations by Stammer and Böning (1992), for example); these will be examined in later papers. Comparisons with eddy estimates from Geosat altimetry are postponed to a later paper because of space restrictions.

2. THE MODEL KINETIC ENERGY

The model (FRAM) is a primitive equation EFGCM. A more detailed description is given by the FRAM group (1991). The resolution in the horizontal is approximately 27 km and as such is the highest resolution primitive equation model of the Southern Ocean run to date. The seasonal climatological winds of Hellerman & Rosenstein (1982) drive the ocean at the surface. The model initially took the climatological hydrography of Levitus (1982) and assimilated it to produce a dynamically consistent set of fields, namely temperature, salinity and velocity. After six years, the assimilation was removed, and the model ran freely, being relaxed back to annual averages of the Levitus temperature and salinity only at the surface. For four years, the model had harmonic mixing and linear bottom friction; for the next six (from where our data are derived) with biharmonic lateral mixing and quadratic bottom friction. These last six years were almost statistically steady, albeit with a slight tendency toward spindown.

The model appears to reproduce many of the known features in the Southern Ocean extremely well. The high resolution enables the model to resolve marginally some of the small-scale synoptic and mesoscale eddies found in the ocean. Fronts, meanders, jets and lenses are all produced internally by the dynamics. Thus from a smooth initial climatology a rich high resolution database has been produced. As such FRAM represents a new and non-conventional technique for examining the dynamics of the Southern Ocean.

The kinetic energy distribution can be described in three ways. The total kinetic energy (TKE) is defined as

$$\text{TKE} = \frac{1}{2}(\overline{u^2 + v^2})$$

where u and v are velocity components east and north respectively.

Of more interest are the two components of the total kinetic energy. The kinetic energy of the mean flow (MKE) is

$$\text{MKE} = \frac{1}{2}(\overline{u^2} + \overline{v^2})$$

and the kinetic energy due to transient eddies (EKE) is

$$\text{EKE} = \text{TKE} - \text{MKE} = \frac{1}{2}(\overline{u'^2 + v'^2})$$

In the above $\overline{\quad}$ represents a time average of u and $u' = u - \overline{u}$ represents the deviation from the time average. The above three quantities have been calculated at every grid point in the model, using 72 instantaneous dumps one month apart. This gives a much

finer spatial representation of the kinetic energy field than has previously been available. We have examined the statistics of this averaging process and are satisfied that the averages we present are robust, and that the separation in sampling time gives effectively statistically independent samples.

The mean flow from FRAM was discussed by Killworth (1992). Figure 1*a* shows the MKE corresponding to this flow at 32 m, the depth level immediately below the model Ekman layer; this level avoids contamination by wind drift†. The 'streakiness', or filamentation, noted by Nowlin & Klinck (1986) and the FRAM group (1991) is immediately evident. The width of the filaments (which are well resolved by the model) varies with their position, which is concentrated in a band roughly aligned with the ACC, together with western boundary currents, although the position and orientation of the streaks is much influenced by the bottom topography. Major topographic features, such as the mid-ocean ridge systems, Drake Passage, Crozet and Kerguelen plateaux are regions of intense jets, although the ACC still retains a multiple jet structure in regions of less rugged topography. Away from the ACC, where the eddy kinetic energy is much reduced, the jet-like structure is absent. Much of this jet structure is probably too narrow to be well observed by drifters.

Figure 1*b* shows the EKE at the level just below the Ekman layer. Its basic pattern is similar to that in the previous studies we have referenced and altimeter studies (Daniault & Ménard 1985; Shum *et al.* 1990), but – as we shall see – the ratio of the highest to lowest values is much higher than in those data; much of the EKE field has extremely low variability. The highest values are found in the Agulhas extension, the storm track region leading southeast from S. Africa, in western boundary currents, and in the vicinity of topographic features. In these regions eddies are produced for many different reasons (baroclinic instability, vortex shedding, etc.). Far to the south, the EKE is negligible. In addition to the sources of error discussed later, the deformation radius is much smaller than the grid size at these latitudes.

Figure 2*a* shows how the EKE varies with depth, on a north south section at 150°E. The section is from the eastern coast of Australia to Antarctica. To the north there is a region of high eddy energy in the East Australia (western boundary) Current. Further south another region of high eddy energy occurs in the ACC, where it interacts with the complex topography south of Tasmania. Here high eddy energies penetrate to a greater depth here even though the surface values are lower than those in the East Australia Current. There is a certain amount of bottom trapping (associated with topography of EKE under the ACC and East Australia Current).

The MKE at this section (figure 2*b*) illustrates the multiple jet structure of the ACC particularly well. Once again there is greater penetration with depth in the ACC. The variation in the vertical of both EKE and MKE is well described by the (square of the) first

† Although the surface layer picture is almost identical.

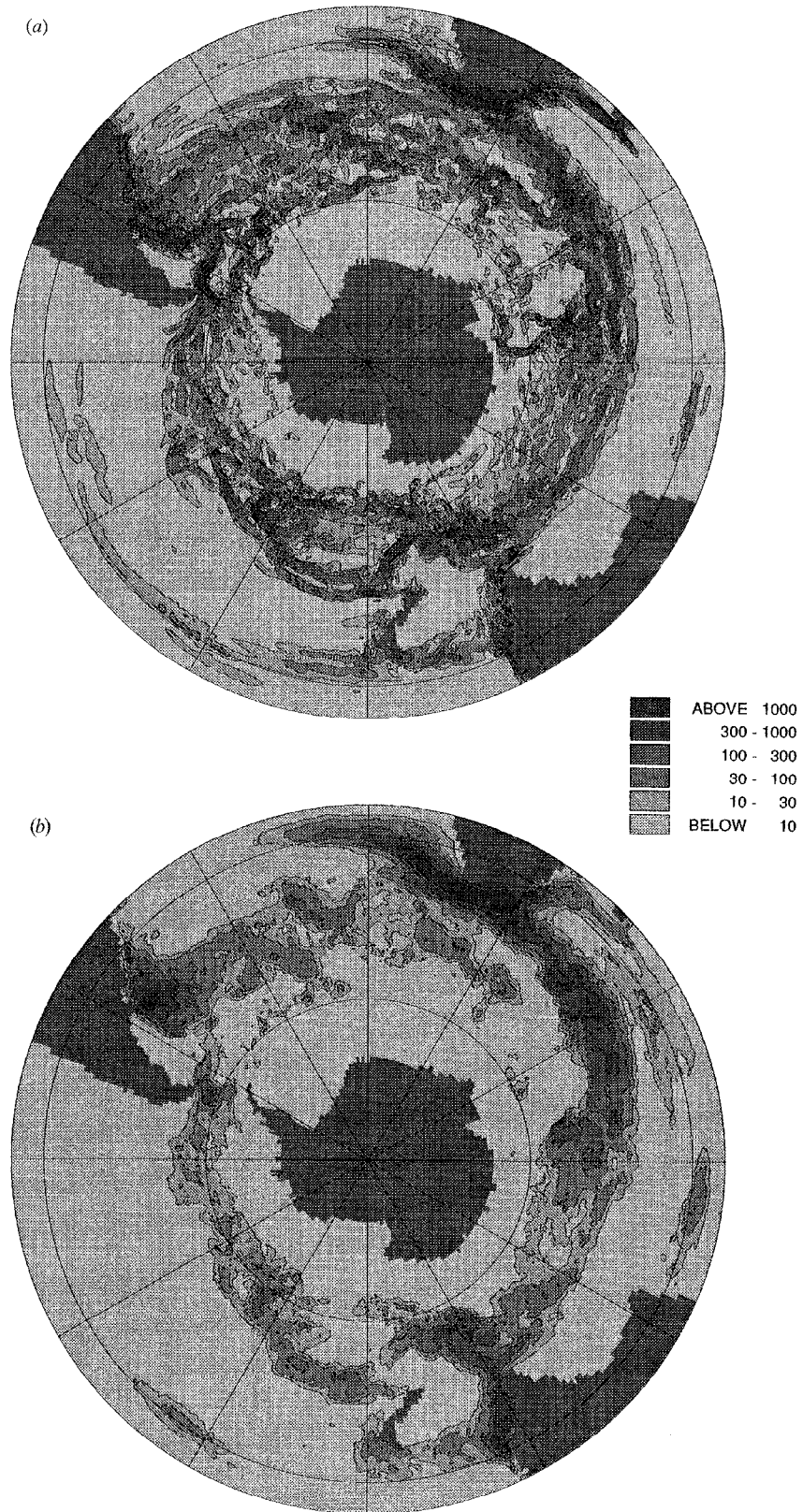


Figure 1. (a) The kinetic energy of the mean flow (MKE) at 32 m depth in FRAM. Contour intervals 10, 30, 100, 300 and 1000 $\text{cm}^2 \text{s}^{-1}$, (b) The mean eddy kinetic energy (EKE) at 32 m depth in FRAM. Contour intervals 10, 30, 100, 300 and 1000 $\text{cm}^2 \text{s}^{-1}$.

empirical orthogonal function discussed by Killworth (1992) for the mean flow.

Accordingly, the EKE and MKE are well correlated. In the surface layer, the correlation is 0.47, which rises to 0.49 in the layer beneath. At 1000, 2000, and 3000 m, the correlations are 0.35, 0.28, and 0.39 respectively (it is unclear why the correlation rises again at depth, although the topography does exercise a degree of control on the flow). Uniformly, the best fit of the EKE as a function of the MKE indicates that EKE levels are, on average, less than the MKE (the amplitude being 0.57, 0.59, 0.15, 0.12, and 0.35 for the five levels reported). Most of the long-term current meter moorings in the Southern Ocean (Dickson 1990) indicate that EKE levels are higher than MKE, although not so noticeably in the Drake Passage. Recall that the locations for current meters were

chosen specially; we shall discuss direct comparisons below. If correlations are performed only over water deeper than 3000 m, then the correlations rise (0.54, 0.55, 0.44, 0.37, 0.39) as do the amplitudes (0.86, 0.87, 0.27, 0.22, 0.35). Thus shallow areas are seen to have different dynamics from deep areas.

It is important to realise that our estimates of EKE have several sources of error, based on missing physics within the model. For example, the model was forced with climatological monthly mean winds, so that variability on more rapid timescales was lacking. This is probably the reason for the very regular occurrence of Agulhas eddies in FRAM, and their repetitive tracks, rather than the more irregular features observed in the ocean. (C. W. Böning, private communication, notes that daily winds made little difference to EKE values in the CME calculations, however.)

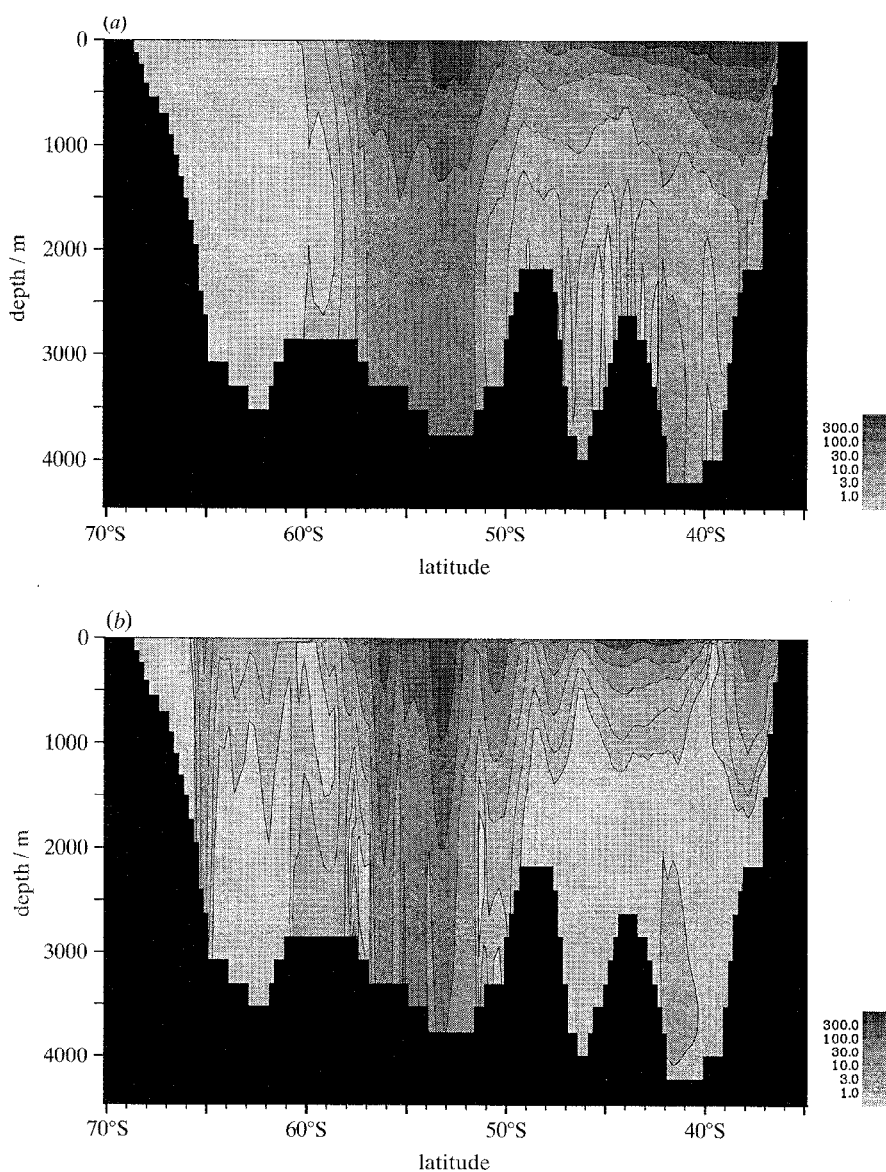


Figure 2. A section of (a) EKE and (b) MKE at 150°E in FRAM. Contour intervals 1, 3, 10, 30, 100 and 300 $\text{cm}^2 \text{s}^{-1}$.

The surface buoyancy forcing involving a relaxation to the Levitus (1982) annual average surface temperature and salinity, so that many baroclinic wave sources are simply not present in FRAM. Another problem was the resolution. Böning & Budich (1992) show that doubling the resolution in their model increased the size of the EKE by factors of at least two (indeed, Barnier *et al.* (1990) demonstrated that high internal modes in quasigeostrophic models are not well represented for grid spacings larger than 10 km), so that we would anticipate an underestimate of EKE in FRAM. Yet another problem is the slightly adjusted topography, which – for example – appears to modify the production of Agulhas eddies (D. J. Webb and J. Lutjeharms, private communication).

3. COMPARISON WITH FGGE DRIFTERS

The FGGE drifter data (provided by S. Patterson) comprised the mean u , mean v , and EKE from the drifters, averaged over 5° squares. Once again the FRAM data were taken from the surface level, the level immediately beneath it, and levels at approximately 1000, 2000, and 3000 m depth. To compare with the FGGE results it was necessary to produce ‘representative values’ for each 5° square from the FRAM data (the comparison is difficult anyway because of the very smooth nature of the FGGE data). We took three possible cases: (i) the value at the centre of the square (actually the mean of the four values straddling it), which we term the local value; (ii) the mean value within the square; and (iii) the median value within the square, to minimise skewing by high values, for example, within the Agulhas region.

These data were then correlated with the appropriate FGGE data. Figure 3 shows results for the level below the Ekman layer. At both the surface and second levels, the local data provided a rather noisy fit with the FGGE data, and the agreement is very poor. However, mean and median data were quite well correlated with the FGGE data ($r=0.67, 0.63$ respectively in the surface layer, and $0.63, 0.57$ respectively in the layer beneath; all are highly significant assuming all data points independent). However, the amplitudes of the FRAM u field were very low compared with the FGGE measurements: the best fit involved an amplitude of only $0.3\ddagger$. Conversely, the v fields were effectively uncorrelated with the data. This might have been expected at the surface, where the direct wind effect would be much more variable in the FGGE data than in the smoothed annual cycle used in FRAM. The EKE was well correlated with observations (0.59 for both mean and median in both layers), but with amplitudes at best 24% of observations.

Good correlations with the FGGE data also occur for lower depths (with reduced amplitudes). In the case of the mean flow, the reason seems to be the equivalent-barotropic nature of the solution (Kill-

\ddagger Danialt & Ménard find, however, that FGGE energies overestimated Seasat energies by a factor of three; even if all corrections were made, the factor was still 1.3. Different measurement techniques simply produce different answers.

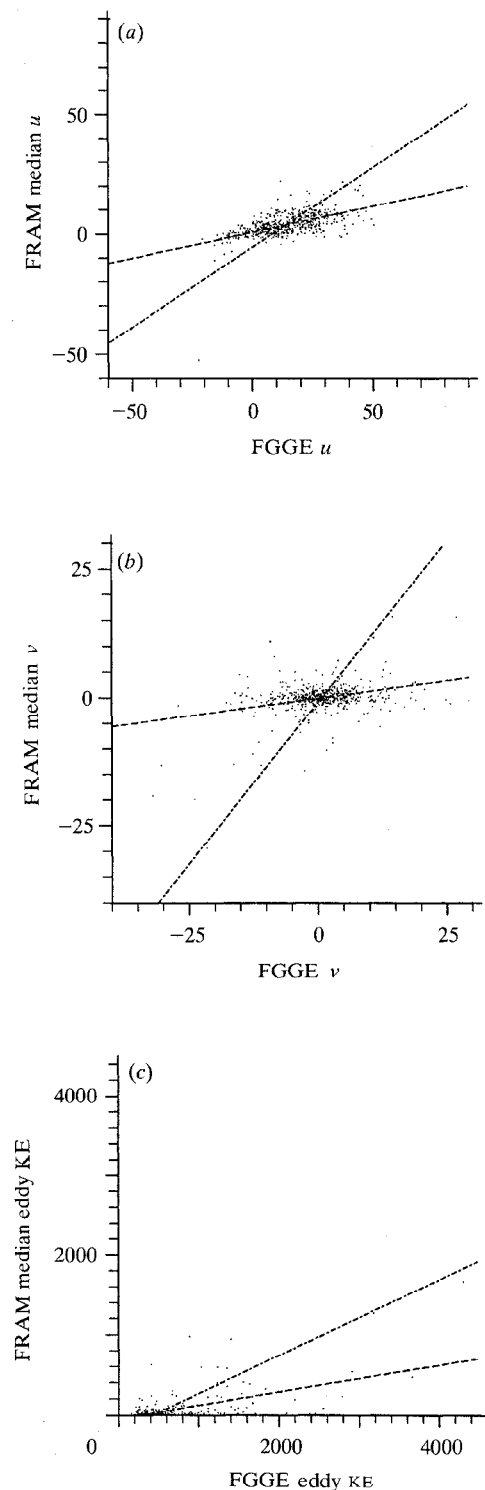


Figure 3. Correlations between FRAM data and FGGE drifter data at 32 m depth. Shown are (a) the mean eastward velocity; (b) the mean northward velocity; and (c) the EKE . The FRAM values are all medians over the 5° square used to compute the FGGE data. The dashed line shows the best linear fit of FRAM on FGGE; the dash-dotted line the reverse. The angle between these lines gives a visual indication of the strength of the correlation. Units are cm s^{-1} .

worth 1992). The square root of the EKE which has units of velocity, has virtually the same structure with depth as the equivalent-barotropic mean flow (found by correlative methods between levels, as well as empirical orthogonal function decomposition).

Curiously, the MKE from FRAM is less well correlated with FGGE MKE than are the individual mean velocities, with correlations of around 0.3 (rising to 0.4 at greater depths). This suggests that where \bar{u} is in good agreement with data, \bar{v} is not, and vice versa. Maps suggest that there is often a slight misplacement of high energy regions by FRAM, probably due to the topographic smoothing employed. This modifies the contours of (Coriolis parameter/depth) which play a fundamental role in the determination of the averaged flow. For example, T. J. Grose (private communication) finds that the northernmost jet in the Drake passage is shifted north of its observed position by the smoothing of the model topography, which has 'eaten into' the coastline.

4. COMPARISON WITH CURRENT METERS

Long-term current meter moorings have been made in seven areas in the Southern Ocean, and summarized by Dickson (1990, *q.v.* for references). A comparison was made with the FRAM data in two ways, similar to how the FGGE comparison was made. We took the values from the nearest FRAM point (in three dimensions) to each mooring, and we also averaged over the nine nearest horizontal points to the mooring. Some data points could not be matched due to different topographies (e.g. the Vema Channel had been filled in by the FRAM smoothing of topography). Correlations were produced ignoring the frequent repetitions of mooring location, etc. The correlations between observations and FRAM overall were:

single point FRAM data: MKE : 0.53; EKE : 0.67.
 nine-point FRAM average: MKE : 0.66; EKE : 0.45.

The differences between these two sets of correlations is statistically significant (as is the size of each correlation), and probably demonstrates that both

data and FRAM energies are spatially highly variable in the eddying regions chosen for current meter moorings. This again points out the difficulty of defining an optimal way to compare models with data. Figure 4 shows the comparison for single point FRAM data; note the apparent double structure for the MKE , with many points having almost no energy in FRAM but large energy in the moorings, and many points for which the opposite holds.

As noted above, the FRAM energies are low compared with observations (although the peak FRAM EKE , over $3000 \text{ cm}^2 \text{ s}^{-2}$, is much larger than the peak EKE observed, $1350 \text{ cm}^2 \text{ s}^{-2}$; both were in the Agulhas region, but at different location). The lowest FRAM energies (both EKE and MKE) are essentially zero. The best fits corresponding to the correlations are

single point FRAM $\text{MKE} = 12.62 + 0.54$ (mooring MKE)
 single point FRAM $\text{EKE} = -17.95 + 0.40$ (mooring EKE)
 nine-point FRAM $\text{MKE} = 18.96 + 0.58$ (mooring MKE)
 nine-point FRAM $\text{EKE} = -28.79 + 0.86$ (mooring EKE).

Note the negative offsets for EKE , produced by many FRAM regions of very small ($0.01 \text{ cm}^2 \text{ s}^{-2}$) EKE , e.g. near the Ross Ice Shelf.

The correlations differ strongly between regions. Southeast of New Zealand, for example, both correlations are above 0.8, although the model EKE has only 14% of the amplitude of that observed. In the Agulhas region, the agreement for EKE is only reasonable (a correlation of 0.36) whereas that for MKE is good (0.81), with both amplitudes above 0.6. However, in the Drake Passage correlations are lower (0.45 for EKE , 0.17 for MKE) as are amplitudes (0.16, 0.29 respectively). Correlations in the S. Atlantic and the Weddell Sea are very poor.

An attempt to isolate the effects of varying depth produced little uniform signal. At depths in which there were enough data to justify computing a correlation, the sign of the result could be positive or negative, and no overall statement could be made.

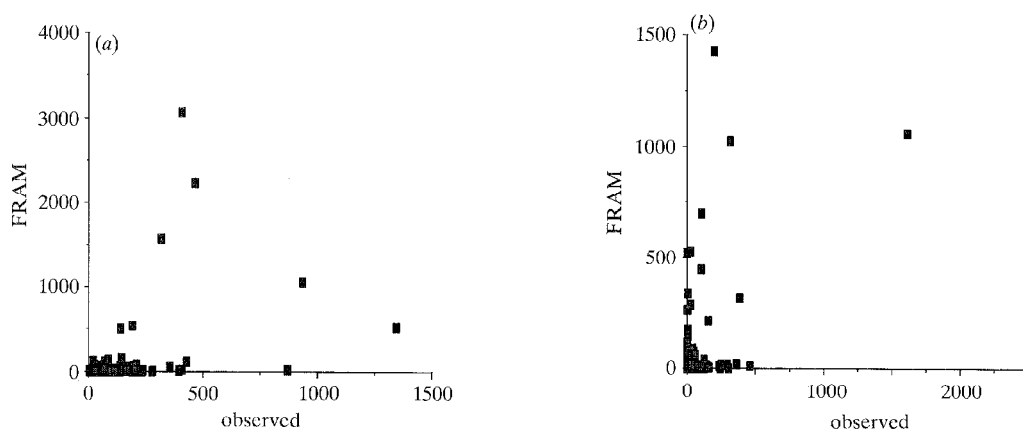


Figure 4. Scatterplot of observed current meter estimates of (a) EKE and (b) MKE , shown against the nearest FRAM grid point estimate. Units are $\text{cm}^2 \text{ s}^{-2}$.

5. CONCLUSIONS

Eddies in FRAM are distributed in a manner similar to, but not identical with, those observed in the Southern Ocean inferred from drifters and current meters (the slight shift in location being probably due to the topographic smoothing employed). Although estimates of energy differ in the data, the model eddies are usually of weaker intensity than those seen in the data (caused by inadequate grid resolution and other reasons). Nevertheless, the correlations suggest that model results may be used as a representation of reality for many purposes.

This work would not have been possible without the help of many members of the FRAM group, in particular the Core Team under David Webb, John Johnson (UEA) and Jeff Blundell (RHI). Our thanks to the late Steve Patterson for providing the FGGE data. The support of NERC grant GST/02/408 is gratefully acknowledged.

REFERENCES

- Barnier, B., Hua, B.L. & Le Provost, C. 1990 On the catalytic role of high baroclinic modes in eddy-driven large-scale circulations. *J. phys. Oceanogr.* **19**, 976–997.
- Böning, C.W. & Budich, R.G. 1992 Eddy dynamics in a primitive equation model: sensitivity to horizontal resolution and friction. *J. phys. Oceanogr.* (In the press.)
- Daniault, N. & Ménard, Y. 1987 Eddy Kinetic Energy Distribution in the Southern Ocean From Altimetry and FGGE Drifting buoys. *J. geophys. Res.* **92**, 11877–11889.
- Dickson, R.R. 1990 Flow statistics from long-term current-meter moorings. The global data-set in January 1989. World Meteorological Office Technical Document, No. 337.
- The FRAM group 1991 An eddy-resolving model of the Southern Ocean. *Eos, Wash.* **72**, 169–175.
- Hellerman, S. & Rosenstein, M. 1982 Normal monthly wind stress over the world ocean with error estimates. *J. phys. Oceanogr.* **13**, 1093–1104.
- Johnson, G.C. & Bryden, H.L. 1989 On the size of the Antarctic Circumpolar Current. *Deep Sea Res.* **36**, 39–53.
- Johnson, M.A. 1989 Southern Ocean surface characteristics from FGGE buoys. *J. phys. Oceanogr.* **19**, 696–705.
- Killworth, P.D. 1992 An equivalent-barotropic mode in FRAM. *J. phys. Oceanogr.* (In the press.)
- Levitus, S. 1982 Climatological atlas of the world ocean (173 pages.) NOAA Prof. Paper 13, U.S. Govt. Printing Office, Washington, D.C.
- Nowlin, W.D. & Klinck, J.M. 1986 The physics of the Antarctic Circumpolar Current. *Rev. Geophys.* **24**, 469–492.
- Patterson, S.L. 1985 Surface Circulation and Kinetic Energy Distributions in the Southern Hemisphere Oceans from FGGE Drifting Buoys. *J. phys. Oceanogr.* **15**, 865–884.
- Piola, A.R., Figueroa, H.A. & Bianchi, A.A. 1976 Some Aspects of the Surface Circulation South of 20°S Revealed by First GARP Global Experiment Drifters. *J. geophys. Res.* **92**, 5101–5114.
- Shum, C.K., Werner, R.A., Sandwell, D.T., Zhang, B.H., Nerem, R.S. & Tapley, B.D. 1990 Variations of Global Mesoscale Eddy Energy Observed from GEOSAT. *J. geophys. Res.* **95**, 17865–17876.
- Stammer, D. & Böning, C.W. 1992 Mesoscale variability in the Atlantic Ocean from Geosat altimetry and WOCE high resolution modelling. *J. phys. Oceanogr.* (In the press.)
- Webb, D.J., Killworth, P.D., Coward, A. & Thompson, S. 1991 The FRAM Atlas of the Southern Ocean. Natural Environment Research Council, Swindon, U.K.
- Wolff, J.-O., Maier-Reimer, E. & Olbers, D.J. 1991 Wind-driven flow over topography in a zonal β -plane channel: A quasigeostrophic model of the Antarctic Circumpolar Current. *J. phys. Oceanogr.* **21**, 236–264.
- Wyrtki, K., Magaard, L. & Hager, J. 1976 Eddy Energy in the Oceans. *J. geophys. Res.* **81**, 2641–2646.

Discussion

C. A. HINDMARSH (*British Antarctic Survey, Cambridge, U.K.*). Is eddy-shedding an inherently unpredictable process? Would this mean that ocean climate itself is inherently unpredictable, or can we hope to work with eddy statistics?

P. D. KILLWORTH. Little is still known about the dynamics of eddy-shedding, and aspects of it may well be unpredictable. However, eddy statistics may be adequate to work with, once we know which ones are applicable. As to ocean climate, simple models suggest that the current state of the ocean may be fairly near a ‘flip-flop’ between two states that bear similarities to ‘strange attractors’.

C. L. PARKINSON (*NASA Goddard Space Flight Centre, Maryland, U.S.A.*). Bert Semtner and Robert Chervin have recently published results from another very impressive high-resolution, eddy-resolving model. Is Dr Killworth aware enough of the details of their work to make some comparisons between their model and his, in terms, say, of model resolution and model physics? Also, is he able to predict at this point any types of differences he might expect in his results versus theirs once one expands to a global mode?

P. D. KILLWORTH. Analysis of the results is still underway, of course. Qualitative differences do stand out between FRAM and Semtner–Chervin. For example, S–C find two fronts in the ACC in Drake Passage; FRAM finds (correctly) three fronts, of which two are in the position observed. However, FRAM has twice as many gridpoints north–south as do S–C, so this improvement is not unlikely. Results from the Kiel group suggest that eddy statistics are much better represented as resolution gets finer.

D. I. M. MACDONALD (*British Antarctic Survey, Cambridge, U.K.*). Dr Killworth said at the start of his presentation that the FRAM model did not include sea-ice cover. He also stated that wind stress was one of the main driving forces of the model. Surely the seasonal sea-ice cover will have a major and annually variable effect on surface wind stress and should be included in his initial model conditions?

P. D. KILLWORTH. Of course, sea-ice should be included from the beginning, rather than only in a single test run, and yes, it does affect the wind stress. The major, if not insuperable, difficulty is that any sea-ice model requires esoterica such as dew point temperatures in the wintertime South Pacific, and we do not have the data to run the model.